Numerical Study of Spin-Spin Correlation and Coherence in dissipative Dicke model

Pascal Würsch
Semester Project, Trapped Ion Quantum Information Group, ETH Zürich
Supervised by: Thanh Long Nguyen & Prof. Jonathan P. Home

October 29, 2019

Abstract

The Dicke model is known for its superradiant phase transition. In dissipative Dicke systems a similar transition can exist. Here we have studied such a dissipative system with individual spin decay. However, the size of the density matrix increases exponentially with number of spins. As the number of spins is increased, the naive approach to solving for the time evolution will rather quickly deplete the computational resources available. By exploiting the systems permutation invariance in spins, the computational workload can be reduced significantly and we are able to evolve systems of up to 7 spins. In the superradiant steady state we find large spin-spin correlations along the x-axis. Further, we make use of the quantum regression theorem to calculate various first and second order coherence functions. For 7 spins, we find that the photonic part of the steady state doesn't deviate much from coherent light.

Contents

1 Introduction

The Dicke Hamiltonian

$$H_{Dicke} = \frac{1}{2}\sum_{i=1}^{N}\omega_a\sigma_z^{(i)} + \omega_c a^\dagger a + g(a^\dagger + a)\sum_{i=1}^{N}\sigma_x^{(i)}. \tag{1}$$

is widely studied and describes the interaction of N identical spin-1/2 systems with a harmonic oscillator [1]. We will refer to excitations of the harmonic oscillator as photons. When $g = 0$, the ground state is the one where all spins point downward and there are no photons. When $g \gg \omega_a, \omega_c$, however, the coupling between spins and photons dominates. In this regime the spins are aligned parallel or anti-parallel to the x-axis. As g is increased the ground state changes (in the thermodynamic limit), meaning there is a phase transition [2],[3].

In dissipative systems a similar phase transition can still occur for the steady state [4]. In this work we consider a system, where the spins independently decay towards the spin down state at rate $\gamma = \gamma_i = 0.1$. When the coupling surmounts a critical value $g_c = \sqrt{\frac{\omega_c(\omega_a^2+(\gamma/2)^2)}{4N\omega_a}}$ [5], the system will relax to a different steady state than below g_c. This is the so-called superradiant phase transition and we will refer to the steady state appearing at g_c as the superradiant phase. More recently, it was shown that a second transition to a non-steady phase with unlimited heating can exist at a coupling about twice as strong as g_c [5]. To describe the evolution density matrices are used. However, their size grows exponentially with the number of spins and hence also the computational cost. An exact method presented by Kirton and Kneeling allows to reduce this scaling significantly [6]. Using this method, we are able to calculate spin-spin covariance and coherence functions for systems of up to 7 spins. Nonetheless, the calculations use computational resources by far exceeding the ones supplied by common home computers (as of today). Therefore, the computations are executed on ETHZ's Euler Cluster, using 30 CPU's in parallel and a memory storage of up to 180GB. The system consisting of 7 spins took roughly 19hrs.

2 Methods

For the following discussion on the Lindblad master equation and quantum regression theorem, we closely follow [7]. If the initial state of the open system $\rho(0)$ is not correlated with the environment, i.e. the full state can be written as a product state $\rho_{SE}(0) = \rho(0) \otimes \rho_E(0)$ and the state of the environment $\rho_E(0)$ is assumed fixed, the evolution of the system can be described by a one-parameter family of completely positive and trace-preserving maps (CPTP) $\{\Lambda(t)\}_{t\geq 0}$, such that $\rho(t) = \Lambda(t)\rho(0)$. Furthermore, we assume the composition law $\Lambda(t)\Lambda(s) = \Lambda(t+s)$, $\forall t, s \geq 0$ to hold. Physically this can be thought of the dynamics not depending on the history nor on time. The composition law formalizes this statement. Under these assumptions the dynamics of the system is governed by the Lindblad master equation

$$\frac{\partial \rho(t)}{\partial t} = \dot{\rho}(t) = -i[H, \rho(t)] + \sum_i \gamma_i (L_i \rho(t) L_i^\dagger - \frac{1}{2}\Big\{L_i^\dagger L_i, \rho(t)\Big\}) \tag{2}$$

with a (system) Hamiltonian H, rates $\gamma_i \geq 0$ and Lindblad operators L_i (sometimes called jump operators). The Lindblad operators describe the effect of the system's interaction with its environment on the system. The square (curly) brackets denote the commutator (anti-commutator). When all rates $\gamma_i = 0$, the master equation reduces to the von Neumann equation describing closed systems. For closed (i.e. unitary) system the two-time correlation function of Heisenberg operators A and B at times $t+\tau$ and t respectively, can be defined as $\langle A(t+\tau)B(t)\rangle \coloneqq Tr[U^\dagger(t+\tau)AU(t+\tau)U^\dagger(t)BU(t)\rho(0)]$, where $U(t) \coloneqq exp(-iHt)$ the usual unitary evolution operator for a Hamiltonian H. The Hamiltonian is assumed time-independent. For the open system, following the definition, we would have to consider the system together with its environment as one closed system. This is beyond the scope of what we do here. To find a calculable expression, however, we make use of the quantum regression theorem: $\langle A(t+\tau)B(t)\rangle_{qrt} = Tr[A\Lambda(\tau)\{B\rho_S(t)\}]$ (again in Schrödinger picture). This last expression for the two-time correlation converges to the definition in the weak coupling limit. In that case, the dynamics of the open system follows the composition law. Also here, a full treatment is far beyond the scope of this project. Therefore we refer the interested reader to literature on the quantum regression theorem and Markovian quantum systems, such as the one cited at the beginning of this paragraph.

From now on, we take eq. 2 and the quantum regression theorem as granted. The quantum

regression theorem allows us to evaluate the first order coherence function

$$g^{(1)}(t,t+\tau) \coloneqq \frac{\left\langle A^\dagger(t+\tau)A(t)\right\rangle}{\sqrt{\left\langle A^\dagger(t+\tau)A(t+\tau)\right\rangle \left\langle A^\dagger(t)A(t)\right\rangle}} = \frac{Tr[A^\dagger \Lambda(\tau)\{A\rho(t)\}]}{\sqrt{\left\langle A^\dagger A\right\rangle_{\rho(t+\tau)} \left\langle A^\dagger A\right\rangle_{\rho(t)}}} \tag{3}$$

and similarly also the second order coherence function

$$g^{(2)}_\rho(t,t+\tau) \coloneqq \frac{\left\langle A^\dagger(t)A^\dagger(t+\tau)A(t+\tau)A(t)\right\rangle}{\left\langle A^\dagger(t+\tau)A(t+\tau)\right\rangle \left\langle A^\dagger(t)A(t)\right\rangle} = \frac{Tr[A^\dagger A \Lambda(\tau)\{A\rho(t)A^\dagger\}]}{\left\langle A^\dagger A\right\rangle_{\rho(t+\tau)} \left\langle A^\dagger A\right\rangle_{\rho(t)}} \tag{4}$$

for all operators A. If $\rho(t)$ is a steady state of eq. 2, then the denominators simplify further, since $\left\langle A^\dagger A\right\rangle_{\rho(t+\tau)} = \left\langle A^\dagger A\right\rangle_{\rho(t)}$ for $\tau \geq 0$. For later use, let's define $j_x \coloneqq \sum_{i=1}^N \sigma_x^{(i)}$.

2.1 Numerical Simulation

The above discussion laid the groundwork of what we're about to implement on a computer. Firstly, we find a steady state ρ_{ss}, i.e. a state such that $\dot{\rho}_{ss} = 0$ in eq. 2. One approach is to convert the density matrix ρ into a column vector ρ_{vec} by stacking its columns (column-stacking). The evolution is then written in form of a (d^2 x d^2)-matrix $\mathbb{L}$ (the Liouvillian superoperator), where d is the dimension of the Hilbert space. The Liouvillian $\mathbb{L}$ acts on the state vector by left-multiplication $\mathbb{L}\rho_{vec} = \dot{\rho}_{vec}$. An easy but tedious calculation shows that for column-stacking it holds: $A\rho \cong (\mathbf{1} \otimes A)\rho_{vec}$ and $\rho A \cong (A^T \otimes \mathbf{1})\rho_{vec}$ for all operators A. Rewriting eq. 2 and usage of the relations just mentioned, gives

$$\mathbb{L} = -i\mathbf{1} \otimes H + iH^T \otimes \mathbf{1} + \sum_i \gamma_i [(L_i^\dagger)^T \otimes L_i - \frac{1}{2}\{\mathbf{1} \otimes L_i^\dagger L_i + (L_i^\dagger L_i)^T \otimes \mathbf{1}\}]. \tag{5}$$

Note however, that we need to limit the number of photons the Hilbert space can host. Computers can only deal with finite-dimensional Hilbert spaces. This is, we need to truncate the physically infinite-dimensional Fock space of photons to a finite dimension n_{max}. Furthermore, the density matrix has $(2^N n_{max})^2$ complex entries and for the Liouvillian superoperator this number is squared. Hence the entries grow exponentially in number of spins N. For modest $N = 7$ and $n_{max} = 60$ the Liouvillian has more than 3.4e15 complex entries and would use roughly 83′000 TB (!) of storage (assuming 24 bytes per complex number). To reduce these numbers, we can make use of the permutation symmetry (w.r.t. the spins). A more in-depth explanation of the idea is given in [6] and in fact, our code is adapted/extended from the code accompanying this paper (published here[8]). The idea and most important results are explained now. The dissipative system we treat here, is only subject to individual spin decay on each of the N spins (Lindblad operators $\sigma_-^{(i)}$). The rate of decay γ_i is equal for all spins. For the same initial conditions on all spins, solving eq. 2 must therefore result in a permutation symmetric density matrix

$$\left\langle s_1^L ... s_i^L ... s_j^L ... s_N^L\right| \rho \left|s_1^R ... s_i^R ... s_j^R ... s_N^R\right\rangle = \left\langle s_1^L ... s_j^L ... s_i^L ... s_N^L\right| \rho \left|s_1^R ... s_j^R ... s_i^R ... s_N^R\right\rangle \tag{6}$$

for all times. Here $s_i^{L(R)} \in \{|\downarrow\rangle, |\uparrow\rangle\}$ labels the basis elements for each spin and photons are not yet included in the expression. This means, all density matrix elements, that result from each other by permutation of the spin labeling (permutation of subscripts), are the same. Hence, it is enough to only keep a smaller number of elements (compression) and evolve these. After the evolution we can reconstruct all missing density matrix elements by permuting the spin labels (decompression). A word on compression and decompression: Consider an arbitrary square complex matrix with dimension $2^N n_{max}$ respecting permutation symmetry in spins (similarly as in eq. 6, but now including photons). Choose any minimal set of density matrix elements (representatives) that allows to reconstruct all others elements. This set can be arranged in the

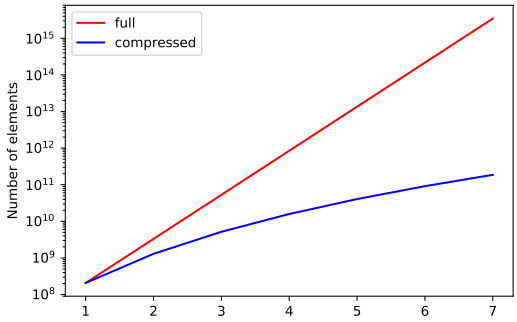

Figure 1: The number of elements in Liouvillian superoperator that describe the evolution without compression (red) and with compression as explained in the text (blue) as function of number of spins N ($n_{max} = 60$). For modest 7 spins the compression achieves a reduction of several orders of magnitude.

form of a vector $M_{comp,vec}$. From this vector we can reconstruct the complete density matrix (as explained below). We have achieved compression and vectorized the matrix M at the same time. The minimal set (in general not unique) and order chosen (for the arrangement into a vector) have no effect on the calculation, other than the need to write the Liouvillian superoperator $\mathbb{L}$ in a form consistent with these choices. For decompression, we need to reconstruct all density matrix elements from $M_{comp,vec}$. All we need to do, is to use eq. 6. We can conveniently extract the density matrix: Multiplication of $M_{comp,vec}$ with an appropriate matrix with $(2^N n_{max})^4$ rows and entries being either 0 or 1, succeeded by an operation reversing the column-stacking. Hence, taking photons into consideration doesn't add much to the complexity. We only need to apply the idea for the compression and decompression scheme n_{max}^2 times - once for each element in a density matrix describing the photon Fock space (dimension n_{max}). With this compression scheme we are able to reduce the number of complex entries in a density matrix to $\binom{N+3}{N} n_{max}^2$. For each spin combine left and right spin indices and encode into a unique number from zero to 3. The cardinality of the minimal set can then be written as a sum of N sums, where each sum runs from zero to the value of the previous index: $n_{max}^2(\sum_{i=0}^{3}\sum_{j=0}^{i}\cdots\sum_{l=0}^{k}1)$. The (reduced) number of entries needed for the density matrix as given above follows. For $N = 7$ and $n_{max} = 60$ this is a reduction from 58'982'400 to 432'000 complex entries! Fig. 1 shows the massive reduction in entries needed for the Liouvillian superoperator and saving these entries corresponds to roughly 4.5 TB of memory. Sparse matrices reduce memory usage even more. The reduction is significant, especially since the system of differential equations has also become much smaller - hence a great reduction of memory usage and computation time.

Now knowing how to compress and vectorize the master equation, we can use a complex ODE solver of choice. We use a 'backward differentiation formula' (BDF) as implemented in the 'scipy.integrate.ode'-class for python. To find a steady state, we evolve the system from an initial condition for 'enough' time steps. How much 'enough' is, depends on the choices made for the Hamiltonian, initial conditions, Lindblad operators and rates. We choose the initial state where all spins point down and there are no photons. Following this recipe, we find a density matrix for each time step, in particular the steady state. This allows us to calculate all possible (same time) expectation values - however not yet coherence functions such as in eqs. 3 and 4. Here we use the quantum regression theorem. For the numerator of these functions, we need to apply the appropriate operator(s) on the steady state by matrix multiplication, compress and take the resulting vector as the initial condition for a new evolution for time τ. Decompression, multiplication with the appropriate operator(s) and taking the trace follows. It is important to recognize, that this compression only works because we choose operators that are permutation

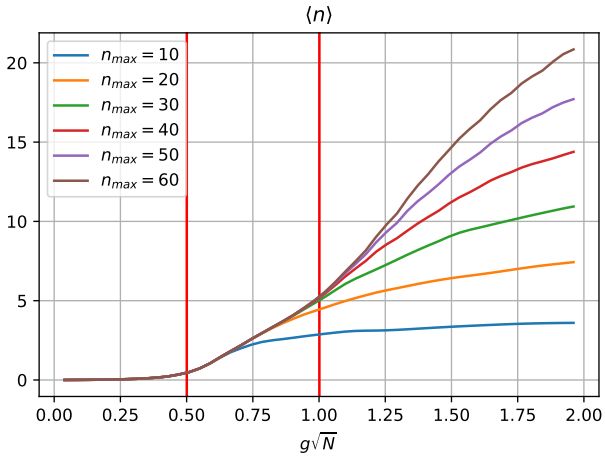

Figure 2: Photon number obtained by simulations with different truncations (7 spins). While the results coincide for low coupling, the truncation strongly affects the obtained solution in the breakdown phase.

invariant in spins, i.e. $j_{\{x,z\}}$ and a. Otherwise, the resulting matrix might not be invariant and hence after compression and evolution one might not be able to faithfully reconstruct the matrix.

3 Results

We have simulated the dissipative Dicke system with individual spin decay (towards the spin down state at rate $\gamma_i = 0.1$, Lindblad operators: $\sigma_-^{(i)}$). As the coupling g increases, we see a sharp rise in the expected photon number. For low enough coupling, the truncation doesn't affect the result of the calculation (fig. 2). For couplings larger than $1/\sqrt{N}$ the results are largely influenced by the chosen truncation. This regime has been identified as a 'non-steady breakdown phase' and does not relax to a steady state [5]. For this influence, we should be careful when interpreting the results in this high coupling regime. Therefore we have marked the two critical couplings (for superradiant and breakdown phase transition) in all figures by two red lines. In the following, we will show, compare and interpret results for 3 and 7 spins ($n_{max} = 60$). All figures will show the results for 3 (7) spins on the left (right). We set $\omega_a = \omega_c = 1.0$. As initial state $\rho_{initial}$ we choose the ground state of the Hamiltonian (eq. 1) with $g = 0$. That is all spins point downward and no photons are in the cavity. From the expectation values in fig. 3 we conclude that the system is in a steady state after at most $t = 50$ time steps (taking into account that the breakdown phase cannot reach a steady state).

3.1 Interpretation

In fig. 4, we can see that the expected photon number as well as the spin expectation value $\langle\sigma_z\rangle$ starts increasing at the critical coupling strength $g_c\sqrt{N} \approx 0.5$. The change of slope at $g_c\sqrt{N}$ is sharper for 7 spins. This is the well-studied superradiant phase transition and is consistent with previous results (e.g. compare with [5], [6]). For $N = 7$ we can see the onset of the breakdown phase transition (at approx. $2g_c$, fig. 2 and 4 (right)).

Evolving from a non-steady initial state, we find that oscillations in spin-spin correlation $cov(\sigma_x^{(i)}, \sigma_x^{(j\neq i)})$ die out more quickly for 7 spins (fig. 5). The spin behavior is governed not only by the Hamiltonian, which is the same for all spins, but also by the individual decay at rate γ_i. The decay for each spin is a stochastic process and hence it is reasonable to see a faster damping of oscillation amplitude for more spins. Further, we find a maximum of correlation in

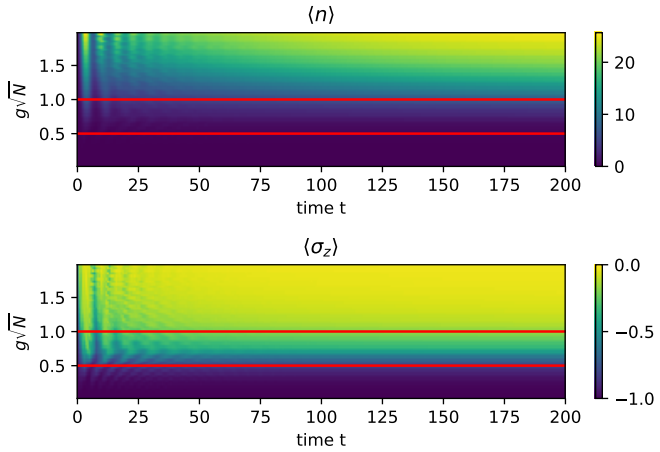

Figure 3: The time evolution of expectation values $\langle n \rangle$, $\langle \sigma_z \rangle$ for 7 spins. The system reaches a steady state for $g\sqrt{N} < 1$ after roughly 50 time steps. For larger couplings the system only reaches a steady state due to truncation.

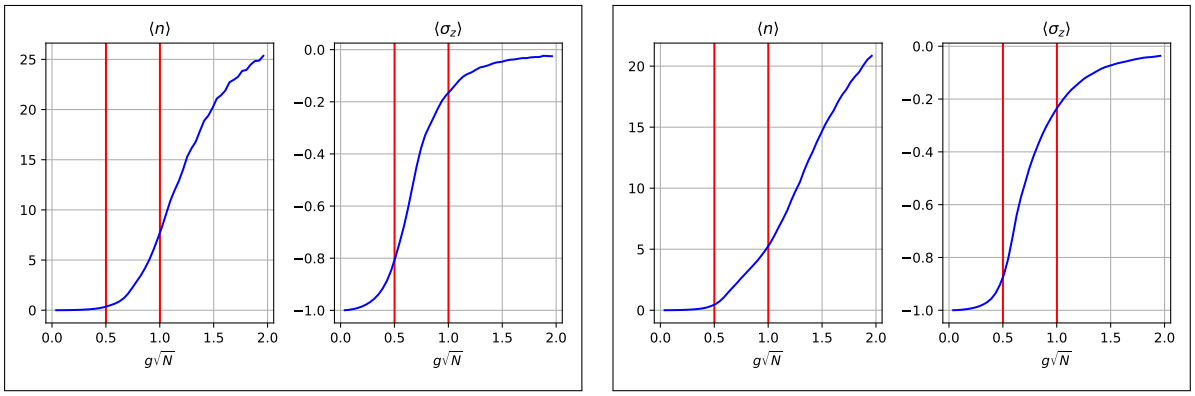

Figure 4: Steady state expectation values $\langle n \rangle$ and $\langle \sigma_z \rangle$ are shown for $N = 3$ (left) and $N = 7$ (right). The steady state changes from a fully polarized state with all spins pointing downwards $\langle \sigma_z \rangle = -1$ ($g = 0$) to a state with only small polarization as the coupling strength is increased.

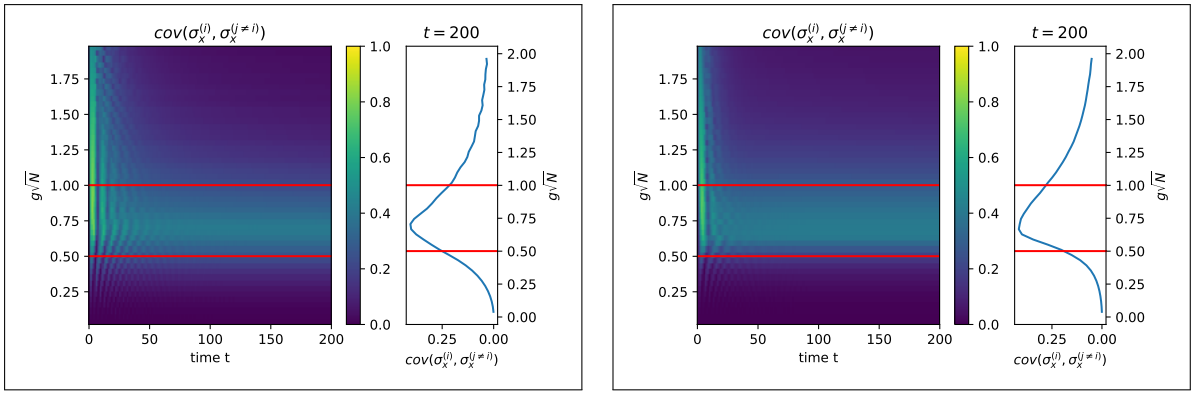

Figure 5: Spin-spin correlation $cov(\sigma_x^{(i)}, \sigma_x^{(j\neq i)})$ of spins on different sites. The relaxation towards a steady state can be observed. For the steady state (i.e. $t = 200$): In the normal and breakdown phase we observe small correlation, whereas in the superradiant phase it reaches its maximum. As the number of spins is increased, the peak changes shape and slightly shifts its position.

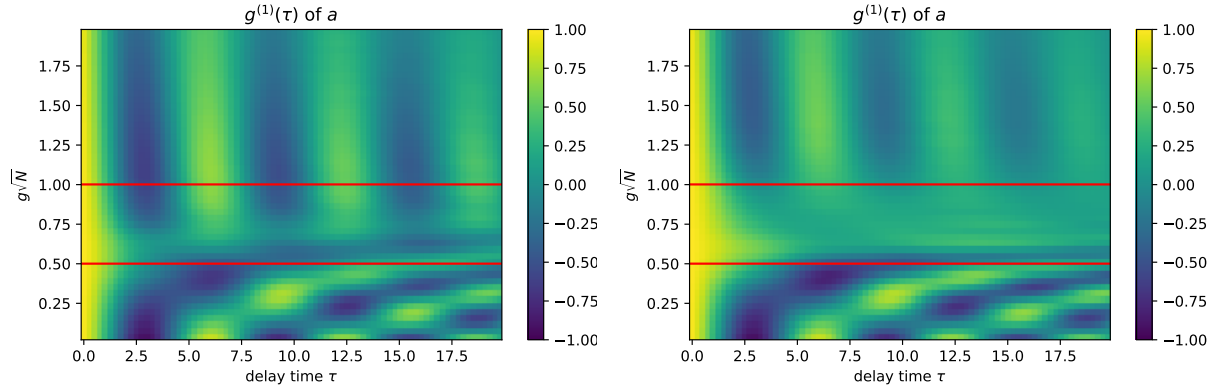

Figure 6: First order coherence function $g^{(1)}(\tau)$ of destruction operator a in steady state. Especially for N=7, there seem to appear qualitative differences between all 3 phases: While the normal phase oscillates differently for different couplings, the breakdown phase oscillates at only one specific frequency. The superradiant phase shows intermediary behavior (N=3) or quick decay to comparably small values (N=7).

the superradiant steady state, which is strictly larger than the values obtained in either of the other two phases (fig. 5). The shape and position of the maximum are slightly different for 3 and 7 spins.

The first order coherence function $g^{(1)}(\tau)$ for photons (fig. 6) looks fundamentally different in all 3 phases: In the normal phase oscillating at frequencies depending on coupling strength while in the breakdown phase only oscillating at one given frequency irrespective of coupling! The oscillation amplitude in the breakdown phase seems to decrease for more spins. In the superradiant phase, for N=3 (left), the system behaves either more like the normal phase or the breakdown phase, depending on the coupling. For N=7 (right), any kind of oscillation is damped rather quickly to a comparably small amplitude.

For $g = 0$ it is clear that the ground state will have $\langle \sigma_x \rangle = 0$, as the state is fully polarized along the z-direction. As our calculation shows, the expectation value $\langle \sigma_x \rangle$ vanishes for all times and couplings. Nonetheless, the first order coherence function of the j_x-operator takes on different values in the normal and superradiant phase and oscillates for couplings smaller than g_c (fig. 7). Now, consider the second order coherence function $g^{(2)}(\tau)$. For the operator j_x (fig. 8), we see some oscillation in the normal phase. In the superradiant phase, we observe a

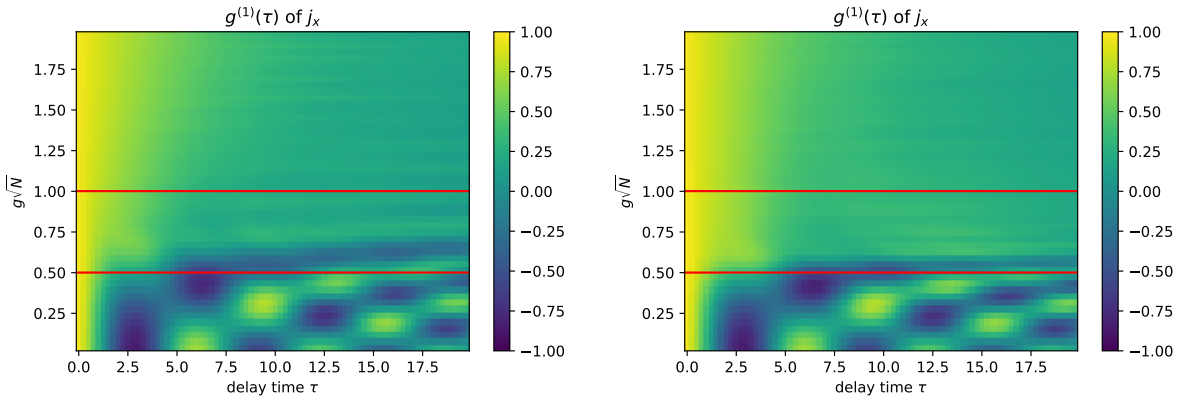

Figure 7: First order coherence function of total spin operator j_x (in steady state). In the normal phase we observe damped oscillations.

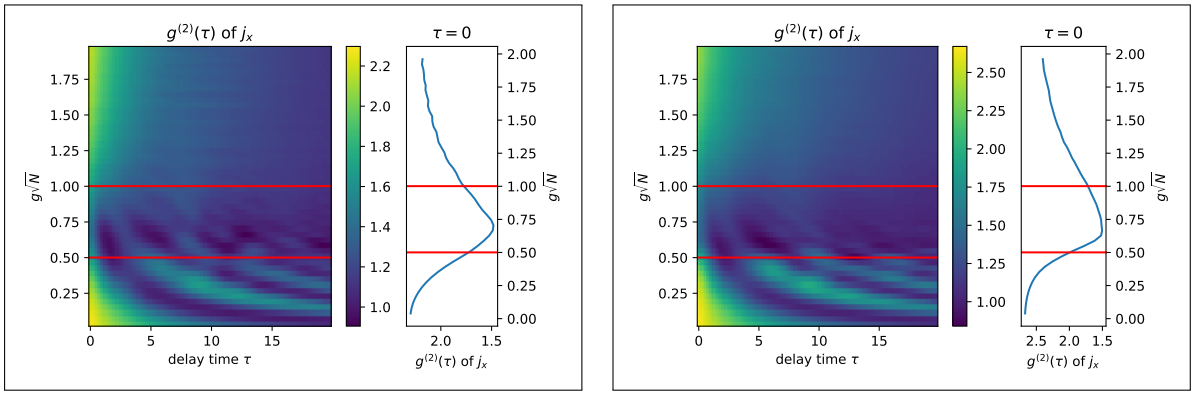

Figure 8: Second order coherence function $g^{(2)}(\tau)$ of j_x in steady state. The correlation function at $\tau = 0$ drops noticeably when entering the superradiant phase to a value of about 1.5. Similarly to observations made for fig. 5, the minima broadens and shifts a bit towards the superradiant phase transition for more spins.

maximum at $\tau = 0$ and a tendency to decrease as τ increases. Similar, to the maximum in spin-spin correlation, we find a minimum in the superradiant steady state, also changing shape and position slightly for different numbers of spin. We are not aware of an accepted interpretation of the second order coherence function for spin operators, as it is usually not applied to such.

In contrast, the photonic second order coherence function has an interpretation as an indicator of how likely it is to measure a photon at time τ given a photon was measured at $\tau = 0$. For coherent light, we expect $g^{(2)}(\tau) = 1$, for anti-bunched light a minima at $\tau = 0$. For small couplings (fig. 9), we see a gradual increase of $g^{(2)}$. In the superradiant phase, the coherence function is closer to a coherent state with values < 2 for all τ and fluctuating comparably close to 1.

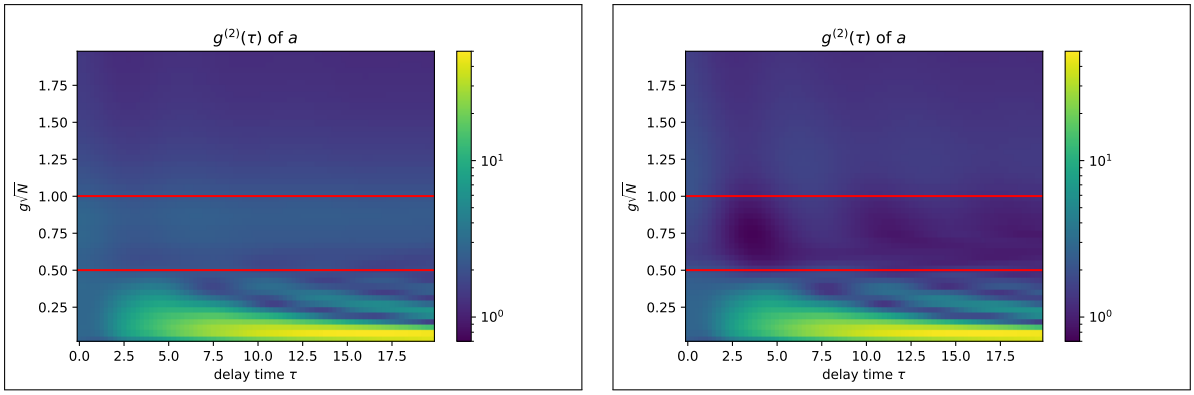

Figure 9: Second order coherence function for destruction operator a. For small couplings ($g \approx 0$) values increase gradually. In comparison, the values in the superradiant phase are fairly close to the value of 1. For 7 spins, there are slight fluctuation around that same value.

4 Conlusion

We have simulated a driven-dissipative Dicke system for up to 7 spins. A compression scheme making clever use of permutation symmetry while still allowing for individual dissipation on the spins was employed. The compression scheme gives a significant reduction of the problem size and only its application allowed us to simulate this many spins on Euler (ETHZ's cluster). Combining the Lindblad master equation and the quantum regression theorem, we have calculated spin-spin correlations and two-time coherence functions (first and second order). In several of our results, we see a qualitative different behavior in the different phases. Namely, the superradiant phase exhibits stronger spin-spin correlation (along the x-axis) than either of the other phases. Correlation is larger for 7 than for 3 spins (in superradiant phase). The second order coherence function of the total spin operator j_x is suppressed in the superradiant steady state. The first order coherence function of the destruction operator a shows differences in periodicity in all three phases. The second order coherence function (of a) for 7 spins fluctuates around 1 in the superradiant phase. For a closed system, i.e. no spin decay, a coherent state is expected (that is a constant value of 1). Hence, it is reasonable to expect a state similar to a coherent state for not too large interaction of the system with its environment.

References

[1] R. H. Dicke, "Coherence in spontaneous radiation processes," *Phys. Rev.*, vol. 93, pp. 99–110, Jan 1954. [Online]. Available: https://link.aps.org/doi/10.1103/PhysRev.93.99

[2] K. Hepp and E. H. Lieb, "Equilibrium statistical mechanics of matter interacting with the quantized radiation field," *Phys. Rev. A*, vol. 8, pp. 2517–2525, Nov 1973. [Online]. Available: https://link.aps.org/doi/10.1103/PhysRevA.8.2517

[3] Y. K. Wang and F. T. Hioe, "Phase transition in the dicke model of superradiance," *Phys. Rev. A*, vol. 7, pp. 831–836, Mar 1973. [Online]. Available: https://link.aps.org/doi/10.1103/PhysRevA.7.831

[4] E. G. Dalla Torre, Y. Shchadilova, E. Y. Wilner, M. D. Lukin, and E. Demler, "Dicke phase transition without total spin conservation," *Phys. Rev. A*, vol. 94, p. 061802, Dec 2016. [Online]. Available: https://link.aps.org/doi/10.1103/PhysRevA.94.061802

[5] F. Reiter, T. L. Nguyen, J. P. Home, and S. F. Yelin, "Cooperative breakdown of the oscillator blockade in the dicke model," *arXiv preprint arXiv:1807.06026*, 2018.

[6] P. Kirton and J. Keeling, "Suppressing and restoring the dicke superradiance transition by dephasing and decay," *Phys. Rev. Lett.*, vol. 118, p. 123602, Mar 2017. [Online]. Available: https://link.aps.org/doi/10.1103/PhysRevLett.118.123602

[7] G. Guarnieri, A. Smirne, and B. Vacchini, "Quantum regression theorem and non-markovianity of quantum dynamics," *Phys. Rev. A*, vol. 90, p. 022110, Aug 2014. [Online]. Available: https://link.aps.org/doi/10.1103/PhysRevA.90.022110

[8] P. Kirton and J. Keeling, "Code accompanying: Suppressing and restoring the dicke superradiance transition by dephasing and decay." [Online]. Available: https://zenodo.org/record/376621#.XVv0uHtCSUk